A Resonant Driver for a Piezoelectric Motor with Single Transistor Direction Switches

Sam Ben-Yaakov[1*], Evgeny Rozanov[1], Tomer Wasserman[2], Tzachi Rafaeli[2], Lior Shiv[2] and Gregory Ivensky[1]

[1] Power Electronics Laboratory, Department of Electrical and Computer Engineering
Ben-Gurion University of the Negev, P. O. Box 653, Beer-Sheva 84105, ISRAEL.
Tel: +972-7-646-1561; Fax: +972-7-647-2949; Email: sby@bguee.ee.bgu.ac.il

[2] Nanomotion Ltd., P. O. Box 223, Yokneam 20692, ISRAEL.
Tel:+972-4-959-0862; Fax: +972-4-959-0995

ABSTRACT

A resonant driver for a Piezoelectric Motor (PZM) is presented, analyzed and tested experimentally. Following a short description of the linear PZM applied in this study, the paper covers the analytical relationships of the buck driven push-pull parallel resonant inverter stage that includes a novel single transistor direction switches. It is shown that the proposed topology is compatible with the drive requirements of the PZM powered from a low voltage (24V). It is also demonstrated that, unlike simple resonant converters, the proposed topology is relatively insensitive to the resonant component values and that it can tolerate added capacitance as introduced when connecting a PZM to the driver via a long cable.

1. INTRODUCTION

Application of piezoelectric (PZ) motors [1, 2] is limited, among other things, by the lack of inexpensive drivers that will match the performance and low cost of the PZ motors (PZM). In this paper we describe a newly developed PZ motor resonant driver that has many advantages over the present solutions. First we describe the linear PZM for which the driver was developed, present its simplified electrical equivalent circuit and give the drive requirement. The classical approach of a series resonant inverter is then covered, pointing to its limitations. We present the proposed Push-Pull Resonant Inverter (PPRI) and derive its basic mathematical operational relationships. We then describe a newly developed PZ motor resonant driver and direction switches that are simpler and hence less costly than previous designs. Finally, we show simulation and experimental results and discuss the merits and drawback of the PPRI and novel single transistor direction switches as compared to the classical series resonant inverter and AC switch approach.

2. THE LINEAR PIEZOELECTRIC MOTOR

The basic operation of the Nanomotion Ltd. (Israel) PZM hinges on the flexure and linear expansion of a PZ slab (Fig. 1). The PZ element has three electrodes, two (A & B) are deposited on one surface (Fig. 1) while the third one (C) is deposited on the bottom surface of the PZ element. Electrodes 'A' and 'B' are of two parts. Each part is placed diagonally on the upper PZ surface (Fig. 1). When an electrical excitation is imposed between 'A' or 'B' electrodes and 'C' electrode, the element will flex and expand and consequently the stem attached to one end of the PZ element, will move in the 'X' and 'Y' dimensions (Fig. 1). Hence, when the PZ element of Fig. 1 is placed against a flat surface as shown in Fig. 2, it will exert mechanical force on the surface and can move the platform if the PZ is mechanically anchored. Excitation of the A-C electrodes will cause movement to one direction while excitation of the B-C electrodes will cause movement in the other direction. For rotary motion the PZM is placed against the circumference of a wheel.

From an electrical point of view, the PZM can be represented to a first approximation by a resonant network (L_s, C_s, R_s) in parallel with the electrical capacitance C_p of the electrodes (Fig. 3a). At the fixed operating frequency, the equivalent circuit can be simplified to a resistor (R_m) in parallel with a capacitor (C_m) (Fig. 3b). This approximation is valid around the operating frequency.

The required motor excitation for full power of the PZ element is 250Vrms at about 40kHz. Being resonant element [1, 2] only the relevant resonant frequencies will develop force. Hence, the ideal drive for the PZM is a sinusoidal waveform since the non relevant harmonics are ineffective and only increase the circulating reactive current. Nonetheless some distortion (30-50%) can be tolerated

* Corresponding author

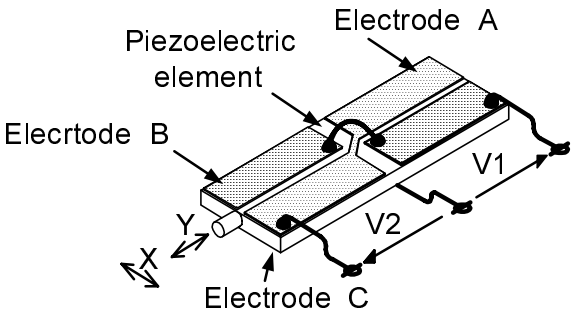

Fig. 1. Electrode configuration in a piezoelectric element of a PZM operating in longitudinal plus flexural mode (Nanomotion Ltd., Israel)

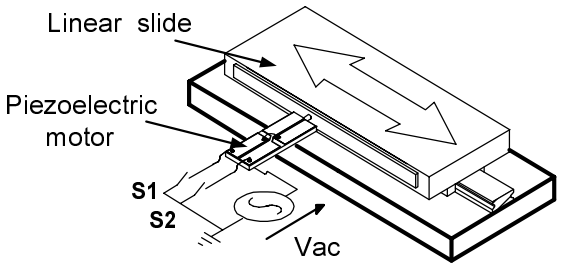

Fig. 2. Method used to generate a linear motion by the piezoelectric element shown in Fig. 1.

without ill effect.

Conventional drivers for a PZM [3] are normally based on a resonant network. In such a configuration the PZM is connected parallel to the capacitor of a series LC-circuit which is fed from the ac network (Fig. 4) or a square wave drive. To achieve a sinusoidal waveform and to obtain a voltage gain, the LC-circuit is normally operated near resonance. In any event, considering the high Q of practical PZM, the power of the motor will be mainly governed by the first harmonic of the drive voltage ($V_{m(1)}$).

In practical cases the cable connecting the driver to the PZM is of variable length and therefore its capacitance C_{cbl} (Fig. 4) may have different values. As a result, the total capacitance $C_\Sigma = C + C_{cbl} + C_m$ is not constant, a fact that might deteriorate the performance of the circuit due to the movement of the resonant frequency.

In an earlier study [4] we derived the dependence of $\frac{\Delta V_{m(1)pk}}{V_{m(1)pk}}$ on $\frac{f_s}{f_{ro}}$ for $\frac{\Delta C_\Sigma}{C_\Sigma} = 0.1$ in the conventional LC

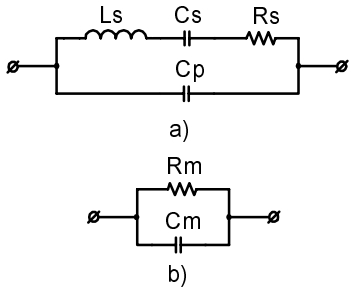

Fig. 3. Equivalent circuit of a piezoelectic element. (a) general circuit for one vibration mode. (b) simplifies equivalent circuit at PZM operating frequency.

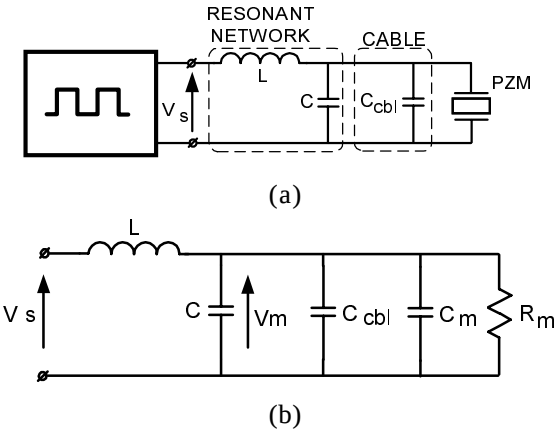

Fig. 4. LC type PZM driver. (a) system configuration. (b) equivalent circuit.

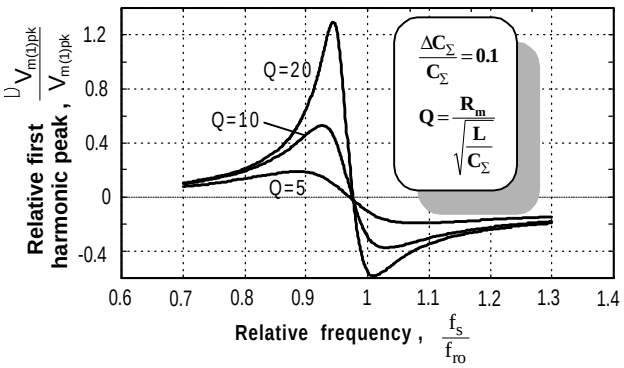

Fig. 5. Output voltage sensitivity of the LC driver to changes in total capacitance as a function of operating frequency. Y axis = relative change in voltage amplitude due to a relative change of 0.1 in total circuit capacitance.

driver (Fig. 5), where f_{ro} is the ideal resonant frequency of the LC_Σ circuit. It is clear that the relative change $\frac{\Delta V_{m(1)pk}}{V_{m(1)pk}}$ can be much higher than $\frac{\Delta C_\Sigma}{C_\Sigma}$, especially at high values of the quality factor Q. However, high Q is needed for good filtering of the square wave normally used as drive and to achieve the voltage gain needed in practical circuits. It is thus clear that the high sensitivity of the output voltage to capacitance changes makes the conventional LC driver useful only when the total capacitances is constant. However, in many practical cases capacitance changes are expected due to many factors: variable cable length, temperature rise of the PZ element which increases its capacitance, practical spread of components' value etc. In these situations, the conventional LC driver is clearly disadvantageous.

3. THE PUSH PULL PARALLEL RESONANT INVERTER (PPRI)

The proposed resonant driver is built around a current fed PPRI [5], [6] and a front end Buck converter (Fig. 6). The function of the Buck converter is to control the average voltage fed to the PPRI and hence the voltage across the motor. The PPRI is run at a constant frequency and the MOSFET switches Q1 and Q2 are driven at 50% duty cycle. The resonant circuit comprises an inductor L, a capacitor C, capacitance of the cable C_{cbl}, capacitance C_m and resistance R_m of the motor (Fig. 6). In practice, the magnetization inductance of the transformer T serves as the resonant inductor L.

The operation of the PPRI can be described by the simplified circuit diagrams of Fig. 7. The input inductor L_{in} (Fig. 6) is replaced here by a current source I_{in} under the assumption:

$$L_{in} >> \frac{4L}{n^2} \qquad (1)$$

where n is the transformer turns ratio. $C2'$, C_{cbl}', C_m', $L2'$ and R_m' are capacitances, inductance and resistance reflected to the primary of the transformer:

$$C2' = \frac{n^2 C}{4} \quad (2); \quad C_{cbl}' = \frac{n^2 C_{cbl}}{4} \quad (3)$$

$$C_m' = \frac{n^2 C_m}{4} \quad (4); \quad L2' = \frac{4L}{n^2} \quad (5); \quad R_m' = \frac{4R_m}{n^2} \quad (6)$$

The drive period T_s must be longer than the resonant period T_r of the real $LC_\Sigma R_m$ circuit:

$$T_s > T_r = \frac{2\pi\sqrt{LC_\Sigma}}{\sqrt{1-\frac{1}{4Q^2}}} \qquad (7)$$

where Q is the quality factor :

$$Q = \frac{R_m}{\sqrt{\frac{L}{C_\Sigma}}} \qquad (8)$$

Each half cycle of the PPRI comprises two operational modes: a resonant mode when one transistor is conducting and both antiparallel diodes are not conducting (Fig. 7b) and a boost mode when the resonant tank is shorted through the conducting transistor and the diode connected antiparallel to the other transistor (Fig. 7c). The duration of the boost mode is dependent on the difference between the drive period T_S and the resonant period T_r. As a result of these two modes, the voltage across the motor v_m will be nearly a sinewave with some dead time between the two half cycles (Fig. 8).

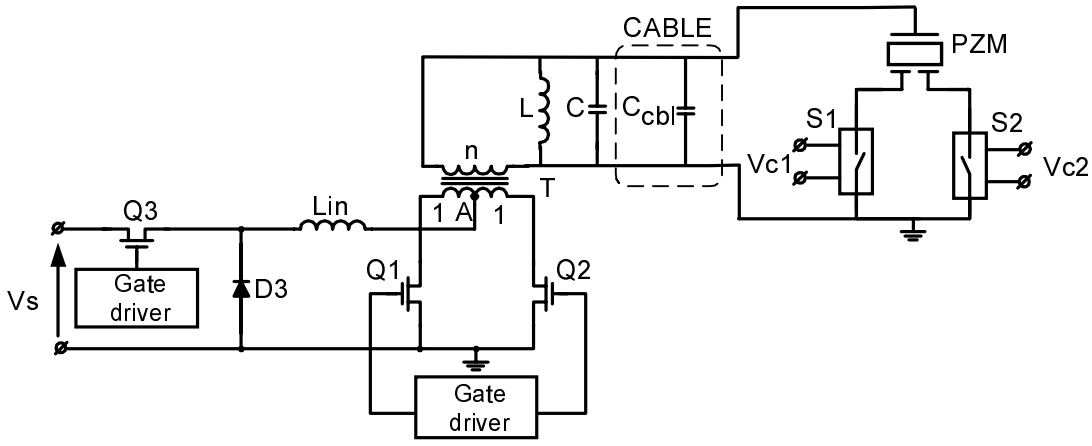

Fig. 6. Basic configuration of proposed PPRI driver. S_1 S_2 control direction of motion (see Figs. 1 & 2).

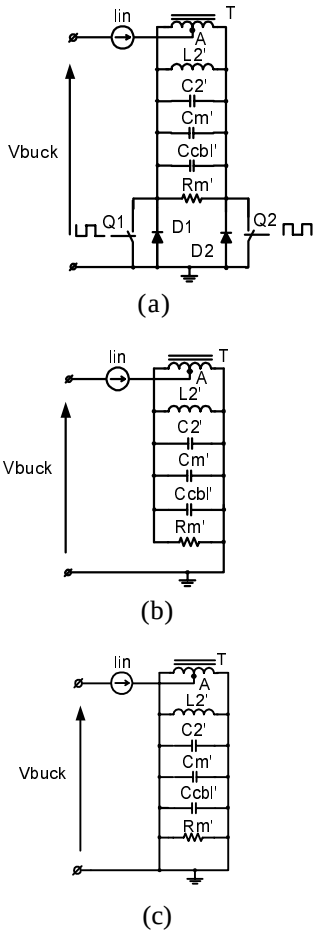

Fig. 7. Equivalent circuit of the PPRI driver (Fig. 6) with the secondary reflected to primary. (a) general circuit. (b) resonant mode. (c) boost mode.

The dead time can be reduced by matching the resonant frequency $f_r = 1/T_r$ to the drive frequency $f_s = 1/T_s$.

We assume that switches, diodes, transformer, inductor and capacitors are ideal and that the waveform of capacitor's voltage (i. e. the voltage across the motor v_m) during the resonant mode is a sinusoidal:

$$v_m = V_{mpk}\cos(\frac{\pi}{\lambda}\vartheta) \qquad (9)$$

where V_{mpk} is the peak motor voltage, $\vartheta = 2\pi f_r t$ is normalized time in radians with zero value when $v_m = V_{mpk}$, t is the time and λ is normalized duration of the resonant mode:

$$\lambda = \pi\frac{T_r}{T_s} = \pi\frac{f_s}{f_r} \qquad (10)$$

The peak motor voltage V_{mpk} is found from the condition that the average voltage across the ideal input inductor L_{in} is zero. Therefore, the average voltage at point 'A' (Figs. 6,7) V_{Aav} is equal to the average voltage across the diode D_3 of the buck converter V_{buck}:

$$V_{Aav} = V_{buck} = D_{buck}V_s \qquad (11)$$

where D_{buck} is the duty cycle of the buck converter and V_S is the supply voltage of the driver (Fig. 6). On the other hand, V_{Aav} can be obtained from (9):

$$V_{Aav} = \frac{1}{\pi}\int_{-\lambda/2}^{\lambda/2}\frac{V_{mpk}}{n}\cos(\frac{\pi}{\lambda}\vartheta)d\vartheta = \frac{2\lambda}{\pi^2}\frac{V_{mpk}}{n} \qquad (12)$$

From (10)-(12) we find:

$$V_{mpk} = nV_{buck}\frac{\pi}{2}\frac{f_r}{f_s} = nD_{buck}V_s\frac{\pi}{2}\frac{f_r}{f_s} \qquad (13)$$

Applying (9) the peak of the first harmonic of the motor voltage can was derived:

$$V_{m(1)pk} = \frac{2}{\pi}\int_{-\lambda/2}^{\lambda}(V_{mpk}\cos(\frac{\pi}{\lambda}\vartheta)\cos\vartheta)d\vartheta =$$

$$= V_{mpk}\frac{4}{\pi}\frac{1}{\pi/\lambda - \lambda/\pi}\cos(\lambda/2) \qquad (14)$$

Taking into account (10) and (13) we transform (14) into:

$$V_{m(1)pk} = nD_{buck}V_s\frac{2\cos(\lambda/2)}{1-(\lambda/\pi)^2} =$$

$$= nD_{buck}V_s\frac{2\cos(\frac{\pi}{2}\frac{f_s}{f_r})}{1-(f_s/f_r)^2} \qquad (15)$$

Eqs.(15) and (7) are used to derive the dependence of $\frac{\Delta V_{m(1)pk}}{V_{m(1)pk}}$ on $\frac{\Delta C_\Sigma}{C_\Sigma}$ (Fig. 5) :

$$\frac{\Delta V_{m(1)pk}}{V_{m(1)pk}} = \frac{[1-(\frac{f_s}{f_r})^2]\cos[\frac{\pi}{2}\frac{f_s}{f_r}\sqrt{1+\frac{\Delta C_\Sigma}{C_\Sigma}}]}{[1-(\frac{f_s}{f_r})^2(1+\frac{\Delta C_\Sigma}{C_\Sigma})]\cos(\frac{\pi}{2}\frac{f_s}{f_r})} - 1 \qquad (16)$$

This relationship is shown in Fig. 9 as a function of $\frac{f_s}{f_r}$

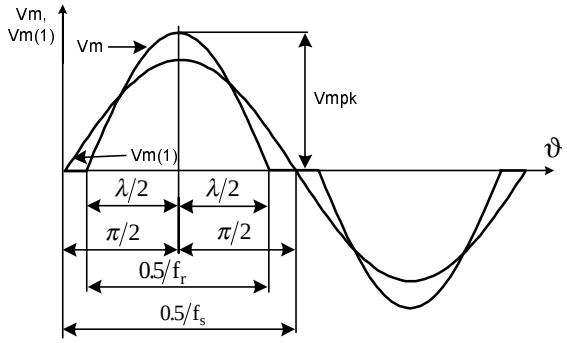

Fig. 8. Output voltage waveform (PZM voltage) of the PPRI driver.

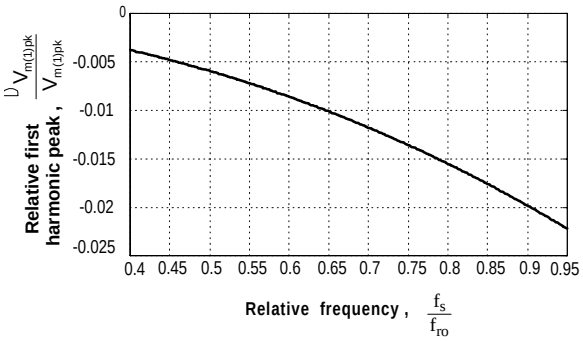

Fig. 9. Output voltage sensitivity of PPRI driver to changes in total capacitance as a function of operating frequency. Y axis = relative change in voltage amplitude of the first harmonics due to a relative change of 0.1 in total circuit capacitance.

for $\frac{\Delta C_\Sigma}{C_\Sigma} = 0.1$. It is seen that in this case $\frac{\Delta V_{m(1)pk}}{V_{m(1)pk}}$ is very small, much lower than $\frac{\Delta C_\Sigma}{C_\Sigma}$. Hence the proposed PPRI topology is clearly advantageous in situations that the capacitance is not constant. That is a very important feature of the proposed driver.

4. THE DIRECTIONAL SWITCH

The direction control scheme of Fig. 6 calls for AC bidirectional switches. A popular realization of such switches is the back-to-back connected two MOSFET transistors configuration (Fig. 10). However, this topology not only requires two transistors but calls for floating gate drives. The solution proposed here is the application of one transistor per switch (Fig. 11). The operation of these AC switches can be understood by considering the relevant equivalent circuit of Fig. 12 when one transistor is on (Q_a) and one transistor is non-conducting (Q_b). Notice that Q_b itself is not affecting the operation of the circuit in the 'off' state, only its diode D_{Qb}. In this equivalent circuit C_t represents the total capacitance at the drain of Q_b, V_{in} is the primary excitation of the driver, while V_{out} represents the voltage of the open PZM terminals. The resonant circuit branches $(L_sC_sR_s)_i$ emulate the electromechanical coupling of the PZM element. A number of resonant branches are considered since the PZM is subjected to multi-mode vibrations.

Considering Fig. 12, it is evident that the operation of the single MOSFET transistor in the present application is controlled by two attributes: (a) the bidirectional conduction capability of the MOSFET when 'on' and (b) the presence of the inherent antiparallel diode. The bidirectional current carrying capability allows AC current to flow through the excited terminals (a-c). The diode does not interfere with the

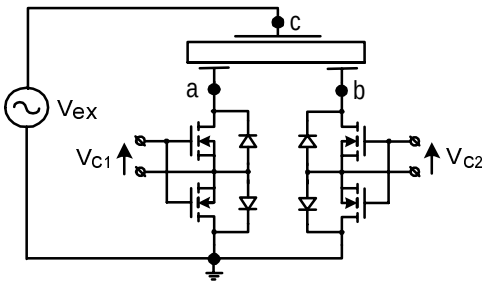

Fig. 10. Direction control by two transistors AC switched.

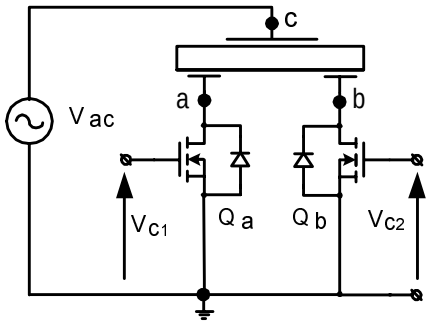

Fig. 11. Proposed single transistor direction switches.

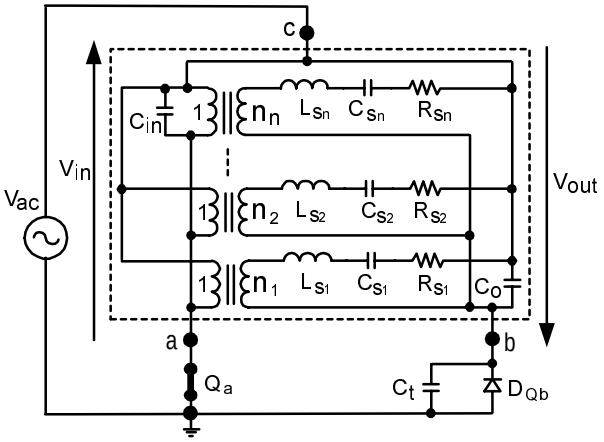

Fig. 12. Equivalent circuit of a PZM controlled by the direction switches of Fig. 11 when Q_a is 'on' and Q_b is 'off'.

blocking requirement for terminal (b-c) since terminal (c) is in fact connected to an unloaded peak detector. Aside from the initial charging current, it will pass no current except for the current through C_t. Note that such a leakage current component will also be present in the classical two transistor AC switch configuration (Fig. 10). The total AC voltage fed to this peak detector is $V_{Qb} = V_{in} + V_{out}$ and hence the expected voltage across the blocking transistor will be the peak to peak voltage of this combined voltage $(V_{Qb})_{pk\text{-}pk}$.

5. RESULTS AND DISCUSSION

A resonant driver was designed for SP1 PZM (Nanomotion Ltd.). The parameters of the PZM were as follows: drive frequency 39.6kHz, maximum drive voltage: 260Vrms, equivalent circuit of PZM: C_m=1.3nF, R_m=3.75kΩ. Nominal supply voltage to driver 24V.

The simulation, analytical and experimental results of the PPRI driver were found to be in excellent agreement. Typical waveforms of the motor voltage are shown in Fig. 13. The robustness of the topology against capacitance changes was tested by adding a capacitance across the PZM. The effect of this extra capacitance on the motor's voltage, motor velocity (Fig. 14) and motor force (Fig. 15) were found to be rather small even when a large capacitance is added (2nF, corresponding to a cable length of 10m).

The experimental results verify the postulated operation of the single transistor AC switch (Fig. 16). The peak voltage of a blocking switch-transistor was found to be about the same as the primary excitation peak voltage.

The results of this study suggest that the proposed PPRI topology is much less sensitive to capacitance variations than the conventional LC driver. Other advantages are also important.

1. In both the conventional LC driver and the proposed PPRI, the relative capacitance change ($\Delta C_\Sigma / C_\Sigma$) can be made small by purposely increasing C_Σ. This however will reduce the characteristic impedance and hence increase the reactive current. The advantage of the PPRI in this case will be in the fact that the circulating current passes through the switches only during the boost period [5]. In the LC driver all the circulating current passes through the switches. Consequently, everything being equal, the PPRI is expected to have a higher efficiency.
2. The incorporation of a transformer in the basic design of the PPRI enables one to use any input voltage to generate the rather high (and floating) voltage needed to drive the PZM.
3. From the electronics point of view, the fact that the drive of the push pull transistors is referred to the 'ground' of the circuit simplifies the design. The circuitry involved is rather simple and can be realized by low cost commercial components.
4. Motor voltage regulation can be easily achieved by just adding an extra switch to form the Buck front end. Motor voltage is linear with the duty cycle, making the control circuitry simple.
5. The proposed single transistor AC switch is much simpler than the conventional two transistor configuration. Aside from the fact that the proposed switching scheme needs half the number of transistors, its drive requirements are easier to meet since the drive signals are referred to ground (Fig. 11).

The main disadvantage of the proposed AC switch is the relatively high peak voltage when the switch is blocking.

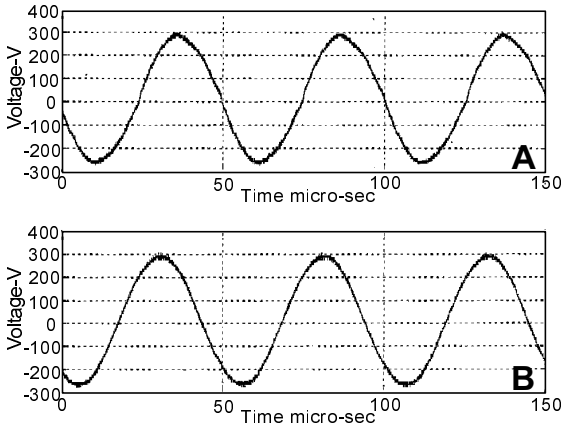

Fig. 13. PZM voltage when driven by proposed PPRI drive. (A) 3 m cable (0.6 nF). (B) 10 m cable (2 nF).

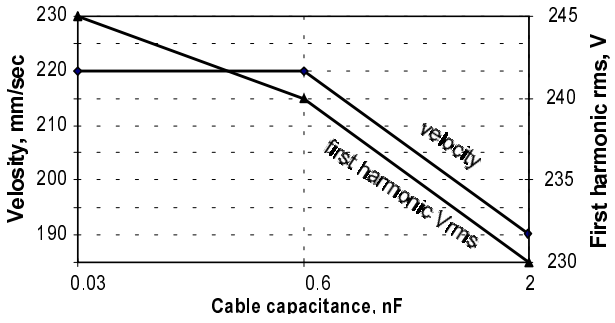

Fig. 14. PZM velocity and rms of first harmonics when driven by proposed PPRI driver, as a function of added capacitance.

6. CONCLUSIONS

The proposed resonant driver is shown to be a viable choice for PZM applications. The main advantages of the proposed PPRI topology is relatively insensitivity to added capacitance, simplicity and ease of control. The mathematical expression developed in this study can

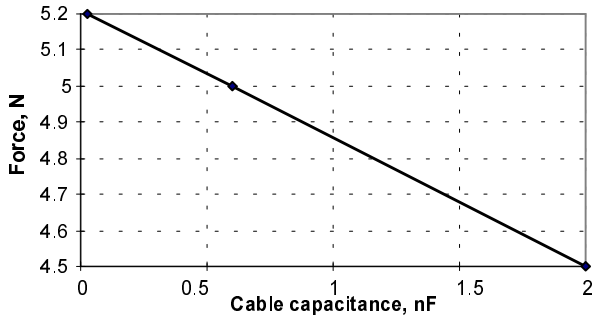

Fig. 15. PZM force when driven by proposed PPRI driver, as a function of added capacitance.

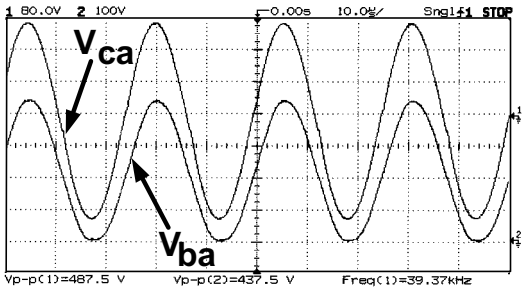

Fig. 16. Excitation voltage (upper trace) and voltage across a blocking direction switch (Fig. 11). Horizontal scale: 10 mSec/div. Vertical scale: 80 V/div, upper trace; 100 V/div, lower trace.

be easily used as design guides for this topology. The proposed single transistor directional switch is simpler and more economical than conventional AC switches. Its main disadvantage is the higher blocking voltage.

REFERENCES

[1] W. R. Chynoweth, J. F. Elliott, H. W. Katz, E. B. Mullen, C. A. Rosen, N. Schwartz, B. Silverman, C. F. Spitzer, S. W. Tehon, H. J. Venema, *"Solid state magnetic and dielectric devices"*, New York, John Wiley & Sons, Inc., 1959.

[2] H.P. Shoner, "Piezoelectric motors and their application," *European Trans. on Electrica Power Engineering*, vol. 2, n. 6, November/December, 1992, pp. 367-371.

[3] Faa-Jeng Lin, "Fuzzy adaptive model - following position control for ultrasonic motor", *IEEE Trans. on Power Electronics*, vol. 12, n. 2, March 1997.

[4] S. Ben-Yaakov, E. Rozanov, T. Wasserman, T. Rafaeli, L. Shiv, G. Ivensky, "A resonant driver for a piezoelectric motor*"*, *Power Conversion and Inteligent Motor Conference*, PCIM'99, vol.39, June 1999, pp.173-178.

[5] G. Ivensky, A. Abramovitz, M. Gulko, S. Ben-Yaakov, "A resonant dc-dc transformer", *IEEE Trans. on Aerospace and Electronic Systems*, vol. 29, n. 3, July 1993, pp. 926-934.

[6] M. Gulko, S. Ben-Yaakov, "Current-sourcing push-pull parallel-resonance inverter (CS-PPRI): theory and application as a discharge lamp driver", *IEEE Trans. on Industrial Electronics*, vol. 41, n. 3, June 1994, pp. 285-291.